# OCCURRENCE OF A WHITE-LIGHT FLARE OVER A SUNSPOT AND THE ASSOCIATED CHANGE OF MAGNETIC FLUX

J. P. LI, M. D. DING and Y. LIU

*Department of Astronomy, Nanjing University, Nanjing 210093, China*
*(e-mail: jpli@nju.edu.cn)*

**Abstract.** A white-light flare (WLF) on 10 March 2001 was well observed in the H$\alpha$ line and the Ca II $\lambda$8542 line using the imaging spectrograph installed on the Solar Tower Telescope of Nanjing University. Three small sunspots appeared in the infrared continuum image. In one sunspot, the infrared continuum is enhanced by 4–6% compared to the preflare value, making the sunspot almost disappear in the continuum image for about 3 min. A hard X-ray (HXR) source appeared near the sunspot, the flux of which showed a good time correlation with the profile of the continuum emission. In the sunspot region, both positive and negative magnetic flux suffered a substantial change. We propose that electron precipitation followed by radiative back-warming may play the chief role in heating the sunspot. The temperature rise in the lower atmosphere and the corresponding energy requirement are estimated. The results show that the energy released in a typical WLF is sufficient to power the sunspot heating.

## 1. Introduction

White-light flares (WLFS) are defined as flaring events that are visible in the optical continuum. They represent the most extreme conditions in solar flares, thereby being of great importance in flare research. According to Machado *et al.* (1986), there exist two extreme types of WLFs: type I that shows a Balmer jump and a hydrogen free-bound (H$_{fb}$) continuum; type II that has no Balmer jump but predominantly a negative-hydrogen (H$^-$) emission. This distinction indicates different energy sources and transport processes in the two types of WLFs. In the case of type I WLFs, the enhanced continuum is closely associated with non-thermal electrons released from the upper atmosphere (e.g., Neidig and Kane, 1993; Neidig *et al.*, 1993; Mauas, 1993; Fang *et al.*, 1995; Liu, Ding, and Fang, 2001; Metcalf *et al.*, 2003); while type II WLFs may originate from a heating source located in the lower atmosphere (e.g., Mauas, Machado, and Avrett, 1990; Ding *et al.*, 1994; Ding, Fang, and Yun, 1999). Despite these differences, one common feature is that the photosphere and the temperature minimum region (TMR), during either type of WLF can be heated to some extent, as is shown in spectral observations and atmospheric modeling of WLFs (e.g., Mauas, Machado, and Avrett, 1990; Ding *et al.*, 1994; Fang *et al.*, 1995). In some situations, such a heating process may extend to the sunspot atmosphere. As a consequence, the sunspot appears to dwindle or finally even disappear in a photographic image.

On the other hand, it is known that the occurrence of flares is associated with magnetic flux emergence and cancellation. Flares are often observed in the vicinity of emerging flux and flux cancellation. The latter is seen as a gradual and mutual decrease of magnetic flux of opposite polarities in photospheric magnetograms (Martin *et al.*, 1984). It is also interesting to study the relationship of magnetic flux cancellation with WLFs.

In this paper, we study a WLF that occurred on 10 March 2001. During this WLF, the atmosphere of a nearby sunspot was gradually heated. This WLF shows also obvious features of emerging magnetic flux and flux cancellation, and is accompanied by the eruption of a coronal mass ejection (Uddin *et al.*, 2004). The paper is organized as follows: we present the observations in Section 2 and show the morphology and evolution of the flare in Section 3; then we discuss the heating of the sunspot atmosphere in Section 4; finally, we draw conclusions in Section 5.

## 2. Observations

This WLF, with Hα/soft X-ray importance 1B/M6.7, occurred at N27W42 ($\mu = 0.63$) on 10 March 2001 and was observed in Hα and Ca II λ8542 lines with an imaging spectrograph in the Solar Tower of Nanjing University. It started at 04:00 UT, peaked at 04:05 UT, and ended at 04:07 UT. A good time correlation between the continuum emission and the microwave radio flux exists, implying that it is a type I WLF. A detailed description of the observations and data reduction can be found in Liu, Ding, and Fang (2001).

This WLF was also well observed by the *Yohkoh* satellite (Ogawara *et al.*, 1991). We use the *Yohkoh* Hard X-ray Telescope (HXT) data to construct the hard X-ray (HXR) image and the time profile, which can provide important information on high-energy electrons. In addition, we use the data from the Michelson Doppler Imager (MDI) on board the *Solar and Heliospheric Observatory* (SOHO) to deduce the magnetic flux evolution associated with this WLF.

## 3. Morphology and Evolution of the Flare

### 3.1. Spatial distribution of flare emission and magnetic topology

Figure 1 displays the contours of the continuum enhancement near the Ca II λ8542 line at different times. The enhancement is defined as $C = (I_f - I_q)/I_c$, where $I_f$ is the continuum intensity at the flare time, $I_q$ is the preflare continuum intensity, and $I_c$ refers to the background continuum intensity (value in the quiet-Sun region). It clearly shows the spatial configuration of the active region: three sunspots can be identified on the continuum image; the continuum enhancement is mainly located in the northeastern region, where a sunspot can initially be seen but later almost disappears; the continuum emission reaches its maximum at ∼04:03:52 UT, with
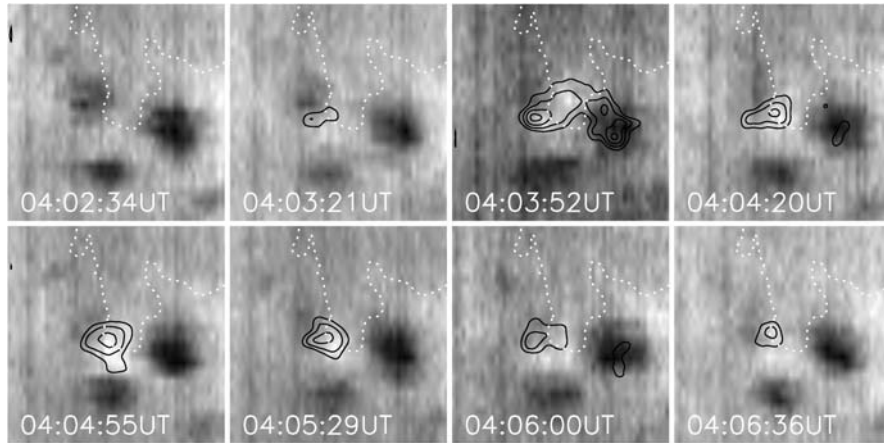
*Figure 1.* Contours of continuum enhancement overlaid on the continuum images. The contour levels are 2.5, 3.5, 4.5, and 5.5%. The *white dotted line* is the magnetic neutral line. The field of view is 50″ × 50″. North is up and east is to the left.

an enhancement of ∼6% compared with the preflare status. To account for this phenomenon, there should be an appreciable heating in the lower atmosphere, under the constraint of pressure balance between the sunspot and the ambient photosphere. In addition, there also appears another patch of continuum enhancement at the site of the western sunspot, which, however, lasts only a short time (see the panel of 04:03:52 UT). These two continuum emission sources look likely the footpoints of a flaring loop. However, it is probably not the case since the durations of the two sources are very different. It may simply represent a remote footpoint at the end of a larger scale loop that interacted with the main flaring site during the impulsive phase (see e.g. Machado *et al.*, 1988a,b).

A further inspection of Figure 1 reveals that the northeastern continuum emission lies across the magnetic neutral line. This phenomenon is similar to the flare of 29 September 2002 (Ding *et al.*, 2003a), in which only one HXR source is resolved that straddles the magnetic neutral line at earlier times. Generally speaking, flares often show double HXR sources because the electrons produced by magnetic reconnection will precipitate downward along the magnetic field lines to both footpoints of the flaring loop. In this case, we think that this continuum emission may also involve two footpoint sources that are too close to be spatially resolved.

It is commonly accepted that flares are powered by the energy stored in the stressed magnetic field. To understand the magnetic configuration of the flare region, we use the high time cadence (1 min) full-disk level 1.8 MDI data, with a pixel size of 1.96″. All magnetograms have been corrected for solar rotation to match the flare peak time. Figure 2 shows a magnetogram at 03:00 UT, which was observed 1 h before the onset of the flare. The sunspot that disappears in the continuum image
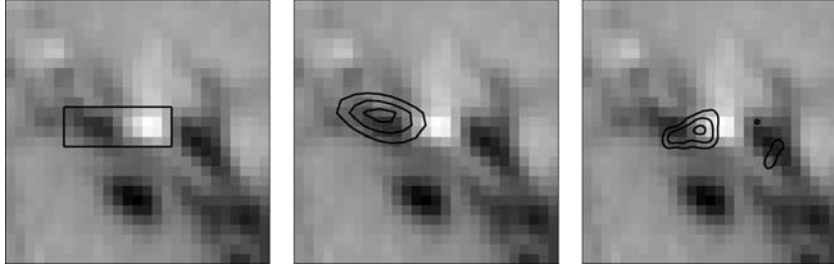
*Figure 2. Left panel*: the black box showing the area of the sunspot for study. *Middle panel*: HXR contours in the 23–33 keV channel from *Yohkoh* with levels of 50, 70, and 90% of the peak intensity. *Right panel*: contours of the continuum enhancement at 04:04:20 UT.

during the flare maximum (marked by a black box) is in fact composed of two areas with opposite magnetic polarities. The other two sunspots have negative polarities.

The middle panel of Figure 2 shows the HXR contours overlaid on the magnetogram, and the right panel shows the contours of the continuum enhancement at 04:04:20 UT. We have used the cross-correlation method to co-align the magnetogram and the continuum images. The correlation is expected to be good to ∼1 MDI pixel in each direction, i.e., ±2 arc sec. The HXR image is constructed using the *Yohkoh* HXT data. As the pointing of the *Yohkoh* satellite is thought to be fairly well known, the HXR image can be directly co-aligned with the magnetograms. By comparing the three panels, we find that there seems to be a slight misalignment existing between the HXR source and the continuum emission source, which straddles the magnetic neutral line. However, we still conjecture that they are spatially consistent, considering the uncertainties due to the limited spatial resolution of each instrument.

## 3.2. TIME PROFILES OF FLARE EMISSION

Figure 3 displays the time profiles of the HXR flux in the first two energy channels observed by *Yohkoh*. The flux in the higher-energy channels (33–53 and 53–93 keV) is not shown, as it bears an evolution similar to that in the 23–33 keV channel. Also plotted are the time variation of the full width at half maximum of the Hα profile (with the preflare profile subtracted) and that of the continuum enhancement, averaged over the marked region in Figure 2. Apparently, these time profiles are correlated with each other at the impulsive phase of the WLF, considering that the time cadence of our observation is 30–40s. Since the width of the Hα line reflects the magnitude of Stark broadening and is thus a good indicator for electron beam bombardment (Fang, Hénoux, and Gan, 1993; Fang, Hénoux, and Ding, 2000), its correlation with the HXR flux implies that energetic electrons may be the main energy input for the sunspot heating.
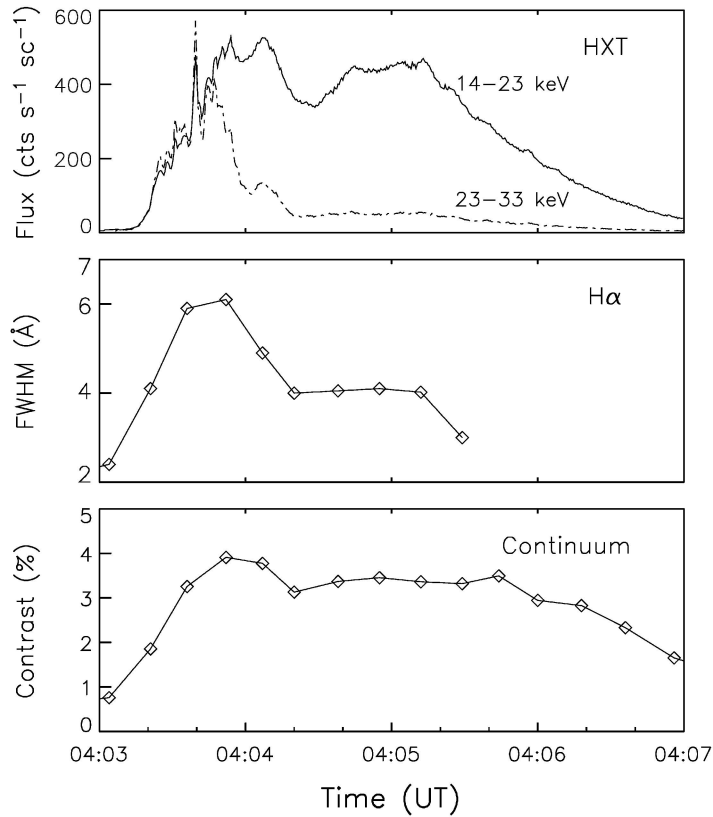
*Figure 3.* Time profiles of the HXR flux in the first two energy channels observed by *Yohkoh*, the full width at half maximum of the Hα emission profile, and near the Ca II λ8542 line continuum enhancement.

### 3.3. EVOLUTION OF MAGNETIC FLUX

Using the SOHO/MDI magnetograms with a time cadence of 96 min, Uddin *et al.* (2004) studied the long-term evolution (from 2 to 10 March 2001) of this active region and found obvious features of magnetic flux cancellation. They pointed out that the process of flux cancellation was a major source of energy build-up. In order to study the magnetic evolution during the flaring time, we further use the high-cadence (1 min) magnetograms. Figure 4 shows the time profile of magnetic flux of the sunspot region marked by a black box in Figure 2, together with the average continuum enhancement in the same region. It is obvious that both the positive and negative flux suffer a very rapid and substantial change during the flare (see Figure 4). The positive magnetic flux shows a fast growth; at the same time, the negative magnetic flux drops coincidently. It is interesting that there is an obvious imbalance between the positive and negative magnetic fluxes before the flare;
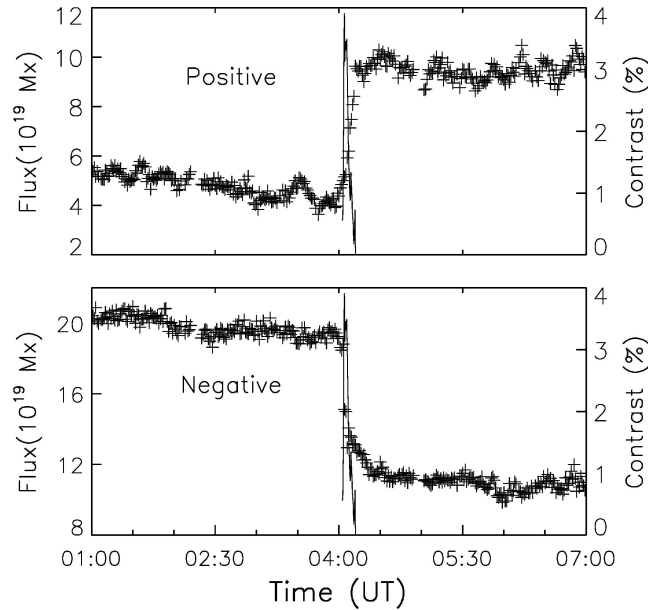
*Figure 4.* Positive (*top panel*) and negative (*bottom panel*) magnetic fluxes in the sunspot as a function of time. Overplotted is the time profile of continuum enhancement (*solid line*).

however, a rough balance is reached after the flare. Transient magnetic field changes associated with solar flares have been observed by ground and space instruments. By making non-LTE calculations, Ding, Qiu and Wang (2002) found that the Ni I 676.8 nm line, used by SOHO/MDI to measure the magnetic field, may appear in emission in the presence of a fairly strong electron beam and preferentially in a sunspot atmosphere. This fact implies that the longitudinal magnetic field observed during some flares may not be accurate. However, if there is no bombarding electron beam, the profile can hardly turn to emission even though the atmosphere is heated to higher temperatures through some other ways. We have calculated the magnetic flux changes from 3 h before the flare to 3 h after the flare. It is shown that the change is permanent as the flux keeps steady for a long time after the flare.

Magnetic flux is often observed to gradually decrease in both polarities as the magnetic fields cancel. However, in this flare the positive and negative magnetic fluxes show contrary changes. This special kind of magnetic field change has been reported by Martres *et al.* (1968). They studied an active region in which all the flares occurred where the magnetic flux was increasing on one side while it was decreasing on the other side of the magnetic neutral line. To account for this phenomenon, a model of an emerging flux followed by a flux cancellation is required.

In summary, the HXR source and the continuum emission are spatially and also temporally correlated. This fact indicates that the sunspot region is the main site of energy deposit. The uncommon change of magnetic flux indicates that this

WLF is triggered by a new emerging flux that induces a flux cancellation. As a result, magnetic reconnection occurs at the upper atmosphere of the sunspot region; thereby high-energy electrons precipitate along magnetic filed lines and deposit energy at the sunspot region, which produce the HXR emission and the continuum enhancement.

## 4. Heating of the Sunspot Atmosphere

### 4.1. THE HEATING MECHANISM

As analyzed earlier, energetic electrons may be the main energy input for the sunspot heating. Electron bombardment on the solar atmosphere, as computed in semi-empirical models (e.g., Aboudarham *et al.*, 1990), has two consequences: an enhanced hydrogen recombination emission and an increased $H^-$ opacity. However, direct heating by an electron beam of the lower atmosphere, where the continuum originates, is impractical since it requires that the energy of the beam electrons to be unrealistically high. Other energy transport mechanisms, such as heat conduction and irradiation by EUV and soft X-rays, also seem inadequate to power the enhanced continuum (Machado, Emslie, and Brown, 1978; Emslie and Machado, 1979; Machado and Hénoux, 1982; Neidig, 1989). On the other hand, Ding *et al.* (2003b) have examined the radiative back-warming effect proposed by Machado, Emslie, and Avrett (1989), and found that it can effectively account for the heating of the TMR and the upper photosphere.

To fully heat the sunspot, an indispensable condition is that the WLF footpoint should be located in or close to the sunspot area. This prerequisite is satisfied as shown in Figure 2 that the continuum-enhanced region is spatially consistent with that of the HXR source. They are both located in the sunspot region. Due to the low electron-energy flux in this WLF (see later), a relatively long time is needed for the radiative back-warming effect to heat the TMR region of the sunspot.

In conclusion, we suggest that electron beam bombardment, followed by radiative back-warming, may be the main mechanism for the sunspot heating.

### 4.2. TEMPERATURE RISE IN THE LOWER ATMOSPHERE

The continuum enhancement in the sunspot region, as described earlier, needs a temperature increase in the TMR and the upper photosphere. To estimate the temperature rise, we perform non-LTE calculations for atmospheric models with modified temperature structures. Based on the VAL-C model atmosphere (Vernazza, Avrett, and Loeser, 1981), we simply lower the temperature in the TMR and the photosphere by 100, 150, and 200 K, respectively, as representing the preflare sunspot atmosphere. Figure 5 displays the contrast at different wavelengths in response to
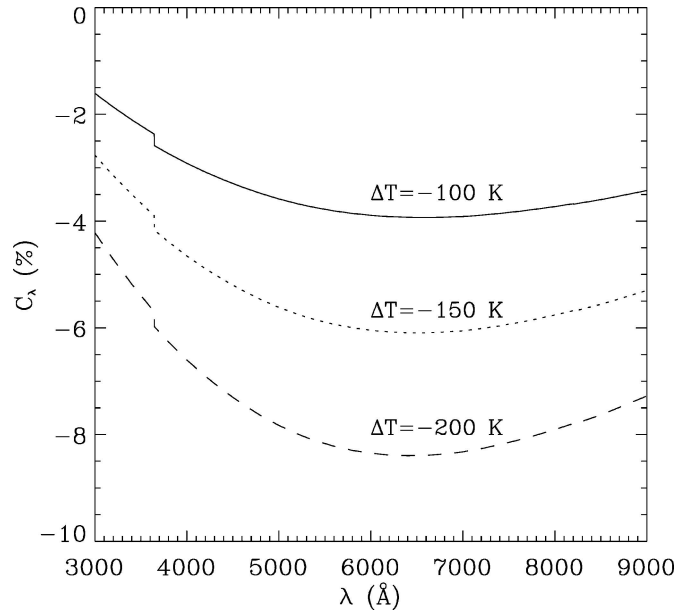
*Figure 5.* Wavelength dependence of the continuum contrast, $C_\lambda$, at $\mu = 0.63$ obtained through non-LTE calculations for different temperature adjustments in the lower atmosphere of the VAL-C model.

the temperature adjustment mentioned earlier. From this figure, we find that the continuum contrast at the Hα wavelength band is most affected by the temperature changes; while the contrast at wavelengths shortward and longward of that band suffers less influence. As the observing wavelength window for the Hα line does not contain the nearby continuum, this result cannot be tested in our observations. Judging from Figure 5, a temperature increase of about 150 K is required to raise the sunspot near-infrared continuum by 4–6% to reach the quiet-Sun level. Because this sunspot is very small and some preflare heating may occur in the sunspot region, it is conceivable that the sunspot lower atmosphere before the flare eruption is only about 150 K cooler than the quiet-Sun atmosphere. This is why we use the simplified model mentioned earlier instead of a standard sunspot model, such as the umbral model of Maltby *et al.* (1986).

### 4.3. ENERGY BUDGET

Because of the lack of broadband spectra, it is rather difficult to quantitatively evaluate the energy required to fully heat the sunspot. As revealed in Section 4, electron bombardment followed by radiative back-warming seems to be the main heating mechanism. Ding *et al.* (2003b) have investigated this issue using numerical simulations. The heating proceeds as follows: at the early phase, an electron beam is accelerated to bombard an unheated atmosphere; radiation from the chromosphere

is greatly enhanced by the bombardment of the electron beam; the photosphere absorbs this radiation and the temperature is increased there, and then the continuum emission rises above the quiescent value, consistent with what is observed. From observations, the total electron energy supplied to the atmosphere could be roughly estimated as

$$\Delta E = \mathcal{F}_1 s \Delta t,$$

where $s$ is the area of the heated sunspot, approximately $6 \times 10^{17}\,\mathrm{cm}^2$ in our measurement of the location where the magnitude of the continuum enhancement exceeds 2% (see Figure 1), $\Delta t$ is the heating time of the sunspot atmosphere that is equal to about 3 min as mentioned earlier, and $\mathcal{F}_1$ is the energy flux of the electron beam. According to the computations of Ding *et al.* (2003b), the present temperature increase requires an energy flux of $\mathcal{F}_1 \sim 5 \times 10^9\,\mathrm{erg\,cm^{-2}\,s^{-1}}$ with an energy cut-off of 20 keV and a spectral index of 4 for the electron beam. From the previous equation, the required energy is computed to be about $5 \times 10^{29}$ erg, smaller than that of a typical WLF (Neidig, 1989). In the present event, this energy comprises only a small part of the total energy released in the whole flare since many areas besides the sunspot are also heated. Hence, this is a good example showing that, during a WLF, the released energy is sufficient to heat a sunspot and to make it disappear in photospheric images.

We should note that the continuum enhancement of 4–6% is only a lower limit, which is affected by the following facts: the spatial resolution of our observations is relatively low, the sunspot size is very small, and the influence of the scattered light is difficult to measure. Therefore, the energy flux of the electron beam actually needed could be larger than the value deduced earlier. Based on the HXR emission observed by *Yohkoh*, Ding *et al.* (2003a) found that, during the impulsive phase ($\sim$04:03–4:04 UT), the power index varies in the range of 3–6. If taking a low-energy cut-off of 20 keV, the energy flux of the electron beam reaches a maximum of $\gtrsim 10^{11}\,\mathrm{erg\,cm^{-2}\,s^{-1}}$. Such an energy flux is over one order of magnitude stronger than the flux that is needed to account for the observed continuum enhancement. We thus conclude that the mechanism of electron beam heating followed by radiative back-warming can nicely explain this WLF even though the observed continuum enhancement is a lower limit.

## 5. Conclusions

We have studied the continuum emission of the 10 March 2001 WLF. The continuum enhancement is mainly located in a sunspot region, so the atmosphere of the sunspot is greatly heated. With the flare development, the continuum emission in the sunspot region reaches the quiet-Sun value within 3 min, showing an increase of 4–6%

relative to the preflare status. This flare also shows evidence of emerging flux and flux cancellation.

The temporal and spatial coincidence of the hard X-ray emission with the continuum emission, shows that electron precipitation may be the main energy source of the sunspot heating. Although the electron beam cannot reach the upper photosphere, radiative back-warming is able to transport the energy deposited in the chromosphere by electrons to the underlying atmosphere. We therefore suggest that electron beam bombardment coupled with the radiative back-warming effect plays the main role in the heating of the sunspot atmosphere.

Through an approximate method, the temperature rise in the sunspot lower atmosphere is estimated to be about 150 K in this event. Based on the results from non-LTE model computations (Ding *et al.*, 2003b), we further obtain the energy input to account for such a temperature increase. The result indicates that it does not challenge the energy requirement for a typical WLF.

## Acknowledgements

## References

Aboudarham, J., Hénoux, J.-C., Brown, J. C., van den Oord, G. H. J., van Driel-Gesztelyi, L., and Gerlei, O.: 1990, *Solar Phys.* **130**, 243.
Ding, M. D., Fang, C., and Yun, H. S.: 1999, *Astrophys. J.* **512**, 454.
Ding, M. D., Qiu, J., and Wang, H. M.: 2002, *Astrophys. J.* **576**, L83.
Ding, M. D., Fang, C., Gan, W. Q., and Okamoto, T.: 1994, *Astrophys. J.* **429**, 890.
Ding, M. D., Chen, Q. R., Li, J. P., and Chen, P. F.: 2003a, *Astrophys. J.* **598**, 683.
Ding, M. D., Liu, Y., Yeh, C.-T., and Li, J. P.: 2003b, *Astron. Astrophys.* **403**, 1151.
Emslie, A. G. and Machado, M. E.: 1979, *Solar Phys.* **64**, 129.
Fang, C., Hénoux, J.-C., and Ding, M. D.: 2000, *Astron. Astrophys.* **360**, 702.
Fang, C., Hénoux, J.-C., and Gan, W. Q.: 1993, *Astron. Astrophys.* **274**, 917.
Fang, C., Hénoux, J.-C., Hu, J., Xue, Y. Z., Gao, X. F., and Fu, Q. J.: 1995, *Solar Phys.* **157**, 271.
Liu, Y., Ding, M. D., and Fang, C.: 2001, *Astrophys. J.* **563**, L169.
Machado, M. E. and Hénoux, J.-C.: 1982, *Astron. Astrophys.* **108**, 61.
Machado, M. E., Emslie, A. G., and Avrett, E. H.: 1989, *Solar Phys.* **124**, 303.
Machado, M. E., Emslie, A. G., and Brown, J. C.: 1978, *Solar Phys.* **58**, 363.
Machado, M. E., Avrett, E. H., Falciani, R., Fang, C., Gesztelyi, L., Hénoux, J. C., Hiei, E., Neidig, D. F., Rust, D. M., Sotirovski, P., Švestka, Z., and Zirin, H.: 1986, in D. F. Neidig (ed.), *The Lower Atmosphere of Solar Flares*, NSO Sunspot, NM, p. 483.

Machado, M. E., Moore, R. L., Hernandez, A. M., Rovira, M. G., Hagyard, M. J., and Smith Jr., J. B.: 1988a, *Astrophys. J.* **326**, 425.

Machado, M. E., Xiao, Y. C., Wu, S. T., Prokakis, Th., and Dialetis, D.: 1988b, *Astrophys. J.* **326**, 451.

Martin, S. F., Bentley, R. D., Schadee, A., Antalova, A., Kucera, A., Dezsö, L., Gesztelyi, L., Harvey, K. L., Jones, H., and Livi, S. H. B.: 1984, *Adv. Space Res.* **4**, 61.

Martres, M. J., Michard, R., Soru-Iscovici, I., and Tsap, T.: 1968, *IAU Symp.* **35**, 318.

Mauas, P. J.: 1993, *Astrophys. J.*, **414**, 928.

Mauas, P. J., Machado, M. E., and Avrett, E. H.: 1990, *Astrophys. J.* **360**, 715.

Maltby, P., Avrett, E. H., Carlsson, M., Kjeldseth-Moe, O., Kurucz, R. L., and Loeser R.: 1986, *Astrophys. J.* **306**, 284.

Metcalf, T. R., Alexander, D., Hudson, H. S., and Longcope, D. W.: 2003, *Astrophys. J.* **595**, 483.

Neidig, D. F.: 1989, *Solar Phys.* **121**, 261.

Neidig, D. F. and Kane, S. R.: 1993, *Solar Phys.* **143**, 201.

Neidig, D. F., Kiplinger, A. L., Cohl, H. S., and Wiborg, P. H.: 1993, *Astrophys. J.* **406**, 306.

Ogawara, Y., Takano, T., Kato, T., Kosugi, T., Tsuneta, S., Watanabe, T., Kondo, I., and Uchida, Y.: 1991, *Solar Phys.* **136**, 1.

Uddin, W., Jain, R., Yoshimura, K., Chandra, R., Sakao, T., Kosugi, T., Joshi, A., and Despande, M. R.: 2004, *Solar Phys.* **225**, 325.

Vernazza, J. E., Avrett, E. H., and Loeser, R.: 1981, *Astrophys. J. Suppl. Ser.* **45**, 635.